



Communication

The competitive and synergistic effect between adsorption enthalpy and capacity in D₂/H₂ separation of M₂(m-dobdc) frameworksFan Wu^{a,b}, Liqiong Li^{a,c}, Yanxi Tan^a, El-Sayed M. El-Sayed^{a,b,d}, Daqiang Yuan^{a,*}^a State Key Laboratory of Structural Chemistry, Fujian Institute of Research on the Structure of Matter, Chinese Academy of Sciences, Fuzhou 350002, China^b University of the Chinese Academy of Sciences, Beijing 100049, China^c College of Chemistry, Fuzhou University, Fuzhou 350108, China^d Chemical Refining Laboratory, Refining Department, Egyptian Petroleum Research Institute, Nasr City, Cairo 11727, Egypt

ARTICLE INFO

Article history:

Received 17 January 2021

Received in revised form 19 February 2021

Accepted 25 February 2021

Available online 27 February 2021

Keywords:

Breakthrough experiment

Open metal sites

Hydrogen isotope separation

Sorption and separation

Chemical affinity quantum sieve

ABSTRACT

Hydrogen isotope separation is a challenging task due to their similar properties. Herein, based on the chemical affinity quantum sieve (CAQS) effect, the D₂/H₂ separation performance of M₂(m-dobdc) (M = Co, Ni, Mg, Mn; m-dobdc⁴⁻ = 4,6-dioxido-1,3-benzenedicarboxylate), a series of honeycomb-shaped MOFs with high stability and abundant open metal sites, are studied by gases sorption and breakthrough experiments, in which two critical factors, gas uptake and adsorption enthalpy, are taken into consideration. Among these MOFs, Co₂(m-dobdc) exhibits the longest D₂ retention time of 180 min/g (H₂/D₂/Ne: 1/1/98) at 77 K because of its second-highest adsorption enthalpy (10.7 kJ/mol for H₂ and 11.8 kJ/mol for D₂) and the best sorption capacity (5.22 mmol/g for H₂ and 5.49 mmol/g for D₂) under low pressure of 1 kPa and 77 K, which make it a promising material for industrial hydrogen isotope separation. Moreover, the results indicate that H₂ and D₂ capacities under low pressure (about 1 kPa) dominate the final D₂/H₂ separation property of MOFs.

© 2021 Chinese Chemical Society and Institute of Materia Medica, Chinese Academy of Medical Sciences. Published by Elsevier B.V. All rights reserved.

As one of the primary nuclear fuels, deuterium (D₂) plays an irreplaceable role in controlled nuclear fusion and is also widely used in non-radioactive isotope tracing, chemical reaction mechanism tracing, as well as medicine and life sciences [1–4]. However, the separation and purification of D₂ from H₂ isotopic mixture is a challenging task due to their similar sizes and chemical properties. Conventional D₂/H₂ separation methods on industrial plant scale, such as cryogenic distillation process and Girdler sulfide process, are highly energy- and time-intensive. Furthermore, these technologies can only provide very low separation factors, making it difficult for extensive application [5–10]. Therefore, it is still an urgent and daunting task to explore new alternative methods for D₂/H₂ separation.

Recently, the strategy of separating hydrogen isotopes based on the kinetic quantum sieving (KQS) and chemical affinity quantum sieve (CAQS) effects of porous materials has attracted considerable attention. Based on KQS effect, which means that different diffusion rates can separate hydrogen isotopes in restricted pores [11], many reports have studied hydrogen isotope separation

behavior of porous materials such as porous carbons [12–15], zeolites [16–18], metal-organic frameworks (MOFs) [19–23], covalent organic frameworks (COFs) [24] and porous organic cages [25]. However, the KQS effect is only obvious at extremely low temperatures (as low as 20 K), increasing separation costs dramatically. Unlike the KQS effect, CAQS effect can effectively separate hydrogen isotopes in porous materials under higher temperatures (≥ 77 K) because hydrogen isotopes demonstrate different adsorption capacity and enthalpies under low pressure [26]. Based on CAQS effect, heavier D₂ preferentially adsorbed on strong active sites, achieving high D₂/H₂ selectivity. Compared to porous carbons, zeolites and COFs, MOFs exhibit more advantages for D₂/H₂ separation because their pore sizes and open metal sites (OMSs) are controllable and further optimize gas uptake and adsorption enthalpy, which are critical factors for D₂/H₂ separation based on CAQS effect. In recent years, MOFs have been widely used in gas separation [27–30]. However, very few MOFs, such as Cu(I)-MFU-4L [31,32], Co-MOF-74 [33] and FJI-Y11 [34], are applied to D₂/H₂ separation based on obvious CAQS effect. Low-temperature thermal desorption spectroscopy indicated that Cu(I)-MFU-4L only showed high H₂/D₂ selectivity at very low temperature (20 K). Furthermore, it is well known that Cu(I)-MOFs are always unstable in air and can be easily oxidized by oxygen, limiting its practical

* Corresponding author.

E-mail address: ydq@fjirsm.ac.cn (D. Yuan).

application. Therefore, we devote to screening stable materials with strong binding sites and high D_2/H_2 uptakes for D_2/H_2 separation under more mild conditions.

Compared to low-temperature thermal desorption spectroscopy, the breakthrough experiment used for D_2/H_2 separation is closer to simulated industrial separation processes. Recently, our group carried out breakthrough experiments to explore D_2/H_2 separation performance of the famous MOF-74 series frameworks with a high density of OMSs, especially Co-MOF-74 that exhibited a satisfying D_2 retention time of 300 min/g ($H_2/D_2/Ne$: 1/1/98) at 77 K [35]. As structural isomers of MOF-74, $M_2(m\text{-dobdc})$ ($M = Co, Ni, Mg, Mn$) frameworks possess a narrower pore size of 9.8 Å than that of MOF-74 (11 Å). The smaller pore size may be more conducive to mass transfer process of hydrogen isotope gas molecules in the channels. Based on the above considerations, we evaluate the D_2/H_2 separation ability of $M_2(m\text{-dobdc})$ frameworks by considering the competitive and synergistic effect between adsorption enthalpy and capacity during the breakthrough process.

$M_2(m\text{-dobdc})$ ($M = Co, Ni, Mg, Mn$) were synthesized by solvothermal method (Fig. S1 in Supporting information) according to previous reports [36]. $M_2(m\text{-dobdc})$ frameworks feature a three-dimensional honeycomb structure constructed by one-dimensional $[M(\mu\text{-COO})(\mu\text{-OH})]_n$ chains. The calculated pore size of $M_2(m\text{-dobdc})$ is 9.8 Å, smaller than that of MOF-74 (11 Å). This facilitates mass transfer process of hydrogen isotope molecules in the channels. Since the hydroxyl oxygen atom and the carboxyl oxygen atom in $m\text{-dobdc}$ ligands are involved in coordination, this series of materials can maintain their original frameworks under high vacuum at 180 °C. The removal of coordinated solvent molecules leaves large number of OMSs, with a calculated density of 4.6 OMSs/nm³ in $M_2(m\text{-dobdc})$, much higher than those of HKUST-1 (2.6 OMSs/nm³) [37] and PCN-16 (1.2 OMSs/nm³) [37]. The purity of prepared frameworks was confirmed by their PXRD patterns (Fig. 1a), and typical type-I N_2 sorption isotherms (Fig. 1b) at 77 K indicate their microporous characteristics.

To better understand the adsorption behavior of hydrogen isotope for $M_2(m\text{-dobdc})$, sorption isotherms of H_2 and D_2 at 77 K and 87 K were obtained, respectively. Among these four materials, $Co_2(m\text{-dobdc})$ shows the highest adsorption capacity as 9.62 mmol/g for H_2 and 10.7 mmol/g for D_2 at 800 mmHg and 77 K, higher than $Ni_2(m\text{-dobdc})$ (H_2 : 8.24 mmol/g, D_2 : 9.24 mmol/g), $Mg_2(m\text{-dobdc})$ (H_2 : 7.97 mmol/g, D_2 : 8.75 mmol/g) and $Mn_2(m\text{-dobdc})$ (H_2 : 7.88 mmol/g, D_2 : 8.56 mmol/g) (Fig. 2). As for the low-pressure part (1 kPa, a partial pressure of H_2 and D_2 during the breakthrough process) of the adsorption curve, the $D_2(H_2)$ adsorption capacity of $Co_2(m\text{-dobdc})$ and $Ni_2(m\text{-dobdc})$ sharply increase to 5.49(5.22) and 4.32(3.96) mmol/g, respectively, which are contrast to the near-flat growth of adsorption curve for $Mg_2(m\text{-dobdc})$ (3.07(2.70) mmol/g) and $Mn_2(m\text{-dobdc})$ (3.29(2.90) mmol/g), which can be attributed to the strong binding force

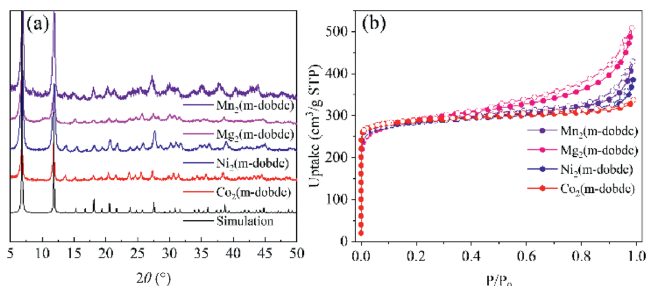


Fig. 1. (a) PXRD patterns of $M_2(m\text{-dobdc})$ ($M = Co, Ni, Mg, Mn$). (b) N_2 adsorption isotherms of $M_2(m\text{-dobdc})$ at 77 K (filled, adsorption; empty, desorption).

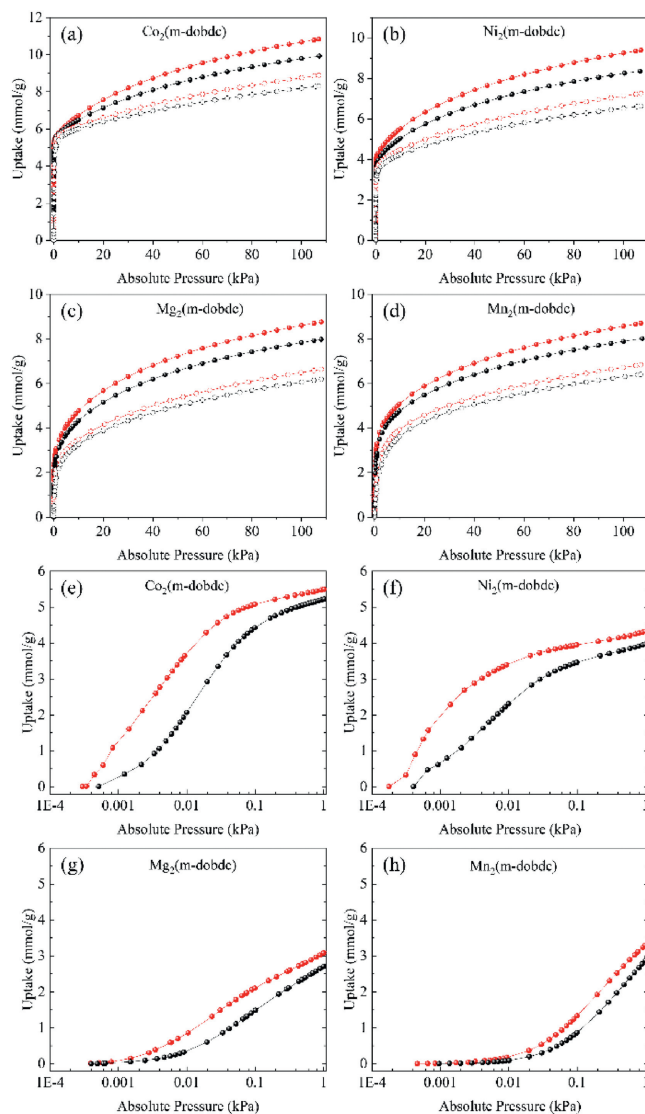


Fig. 2. (a-d) D_2 (red) and H_2 (black) sorption isotherms for $M_2(m\text{-dobdc})$ at 77 K (filled) and 87 K (empty). (e-h) Adsorption isotherms of D_2 (red) and H_2 (black) for pressure in the range of 0–1 kPa (77 K).

between OMSs and hydrogen isotope molecules in the framework. The results further indicate their great potential for D_2/H_2 separation. The results demonstrate that metal centers significantly influence host-guest interactions, resulting in different performance in the selective adsorption of H_2 and D_2 .

Adsorption enthalpy contributes towards understanding the interaction strength between gas molecules and adsorbates. Herein, the adsorption enthalpies of H_2 and D_2 are calculated through the Clausius-Clapeyron equation. As shown in Fig. 3a, among these four materials, $Ni_2(m\text{-dobdc})$ shows the highest adsorption enthalpy of H_2 and D_2 at zero coverage (H_2 : 11.5 kJ/mol, D_2 : 13.0 kJ/mol), slightly higher than $Co_2(m\text{-dobdc})$ (H_2 : 10.7 kJ/mol, D_2 : 11.8 kJ/mol). Such high adsorption enthalpy implies that $Co_2(m\text{-dobdc})$ and $Ni_2(m\text{-dobdc})$ may be good candidates for D_2/H_2 separation.

To predict the D_2/H_2 separation ability of $M_2(m\text{-dobdc})$, the separation performance for $D_2/H_2(50/50)$ mixtures was evaluated through ideal adsorbed solution theory (IAST) [38] (Figs. 3b-e). At 77 K, the $D_2/H_2(50/50)$ selectivity of $Co_2(m\text{-dobdc})$ and $Ni_2(m\text{-dobdc})$ can reach 4.3 and 5.5 at zero coverage, respectively, higher than some famous reported porous materials such as CuBOTf (1.3)

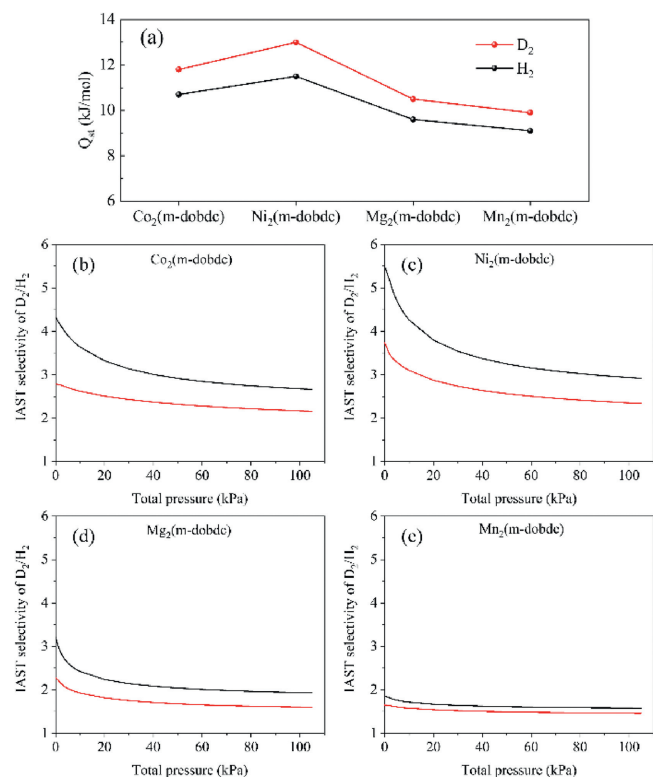


Fig. 3. (a) H_2 and D_2 adsorption enthalpies of $M_2(m-dobdc)$ at zero coverage. (b–e) $H_2/D_2(50/50)$ IAST selectivity of $M_2(m-dobdc)$ at 77 K (black) and 87 K (red).

[39], Fe-MOF-74 (2.5) [26] and Co-MOF-74 (3.2) [26]. When the pressure rises to 1 kPa, these two values still maintain at 4.22 and 5.39, respectively. According to previous reports, materials with such high IAST selectivity at 77 K were rarely reported, meaning the potential ability of $Co_2(m-dobdc)$ and $Ni_2(m-dobdc)$ for separating hydrogen isotopes.

Breakthrough experiments were performed to check the actual separation performance of $M_2(m-dobdc)$. Herein, we simulated two hydrogen isotope mixtures with different compositions ($H_2/D_2/Ne$: 1/1/98) and (H_2/D_2 : 50/50) and evaluated the actual separation ability of $M_2(m-dobdc)$ adsorbents through breakthrough experiments at 77 K and 87 K, respectively. For these four $M_2(m-dobdc)$ adsorbents, when the gas mixture ($H_2/D_2/Ne$: 1/1/98) flowed over the packed column with a flow rate of 15 mL/min at 77 K, H_2 always flowed out first due to its lower adsorption capacity and weaker binding force with adsorbent than D_2 . After the hydrogen broke up, D_2 can still be retained in the packed column filled with $Co_2(m-dobdc)$ for 180 min/g, higher than those of $Ni_2(m-dobdc)$ (150 min/g), $Mg_2(m-dobdc)$ (80 min/g) and $Mn_2(m-dobdc)$ (3 min/g) (Fig. 4). When breakthrough experiments were conducted with $H_2/D_2(50:50)$, effective separation of D_2/H_2 can still be achieved with a breakthrough time of 4.5 min/g for $Co_2(m-dobdc)$ and 3 min/g for $Ni_2(m-dobdc)$, while $Mg_2(m-dobdc)$ and $Mn_2(m-dobdc)$ showed no obvious separation ability. Surprisingly, although $Ni_2(m-dobdc)$ has the highest D_2 and H_2 adsorption enthalpy, $Co_2(m-dobdc)$ showed the longest D_2 retention time. As for $Mg_2(m-dobdc)$ and $Mn_2(m-dobdc)$, they have similar adsorption capacity, but $Mn_2(m-dobdc)$ has inferior separation effect due to its low adsorption enthalpy. The similar rule can also be found in our previous D_2/H_2 separation research on MOF-74. On the other hand, although $M_2(m-dobdc)$ ($M=Co, Ni, Mg$) exhibit similar hydrogen isotope adsorption enthalpies with $M_2(dobdc)$ ($M=Co, Ni, Mg$), $M_2(m-dobdc)$ always showed shorter breakthrough time due to their narrower pore sizes and lower adsorption capacities of

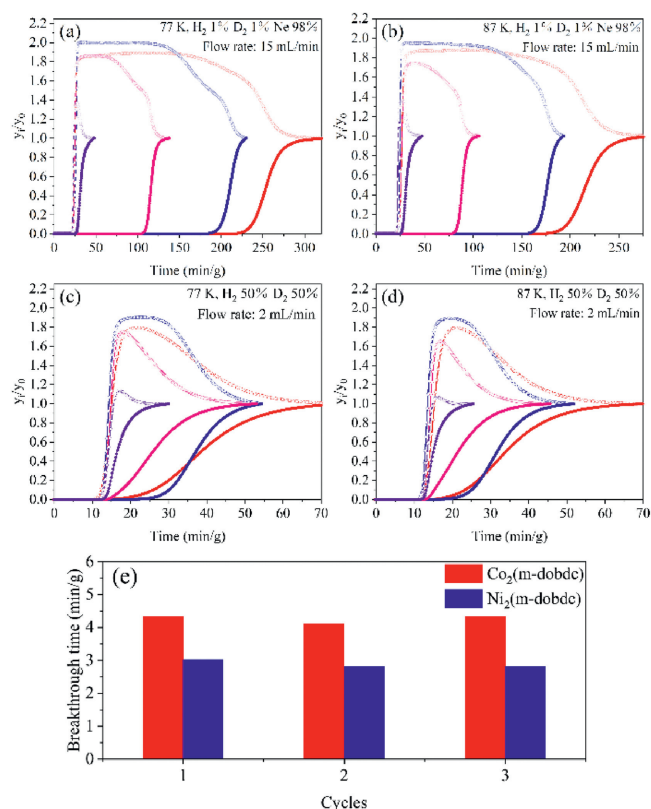


Fig. 4. (a–d) Breakthrough curves for D_2/H_2 separation on $Co_2(m-dobdc)$ (red), $Ni_2(m-dobdc)$ (blue), $Mg_2(m-dobdc)$ (pink), $Mn_2(m-dobdc)$ (violet). The hollow circle represents H_2 , and the solid circle represents D_2 . (e) Breakthrough time of D_2 in cycling tests on $Co_2(m-dobdc)$ and $Ni_2(m-dobdc)$ for $H_2/D_2(50:50)$ mixture.

D_2 and H_2 . Based on the above comparison, although adsorption enthalpy and adsorption capacity are both important to breakthrough experiment performance, adsorption capacity seems to play a more decisive role in D_2/H_2 separation because D_2/H_2 separation conducted by breakthrough experiments requires MOFs to display high D_2/H_2 uptakes as well as significant difference of D_2/H_2 uptakes to extend D_2 retention time. The regeneration of adsorbents is also an important evaluation criterion in industrial applications, and cyclic experiments revealed that during three cycles, the breakthrough times of D_2 in $Co_2(m-dobdc)$ and $Ni_2(m-dobdc)$ remained (Fig. 4e), indicating their excellent cycling stability for D_2/H_2 separation.

In conclusion, D_2/H_2 separation performance of $M_2(m-dobdc)$ is explored by breakthrough experiments, in which two critical factors, including gas uptake and adsorption enthalpy, are considered to investigate the competitive and synergistic effect between adsorption enthalpy and capacity in D_2/H_2 separation ability of $M_2(m-dobdc)$ frameworks. The results showed that for MOF materials with approximate adsorption enthalpies, MOF with higher gas uptake exhibits greater D_2/H_2 separation performance. Therefore, among these materials, $Co_2(m-dobdc)$ exhibits the second-highest hydrogen isotope adsorption enthalpy and the highest gases uptake (5.22 mmol/g for H_2 and 5.49 mmol/g for D_2) under 1 kPa, making it the best material for D_2/H_2 separation with D_2 retention time of 180 min/g for ($H_2/D_2/Ne$: 1/1/98) at 77 K. Compared to Co-MOF-74 (Table S1 in Supporting information), $Co_2(m-dobdc)$ has lower adsorption enthalpy and capacity, resulting in shorter retention time of D_2 . The results demonstrate that the adsorption capacity shows a more significant impact than adsorption enthalpy on D_2/H_2 separation performance. This work

demonstrates a noteworthy design consideration to develop materials with excellent hydrogen isotope separation ability.

Declaration of competing interest

The authors declare that they have no known competing financial interests or personal relationships that could have appeared to influence the work reported in this paper.

Acknowledgments

This work was financially supported by the Strategic Priority Research Program of Chinese Academy of Sciences (No. XDB20000000), the Key Research Program of Frontier Sciences, Chinese Academy of Sciences (No. QYZDB-SSW-SLH019) and the National Natural Science Foundation of China (Nos. 21771177, 51603206 and 21203117).

Appendix A. Supplementary data

Supplementary material related to this article can be found, in the online version, at [doi:https://doi.org/10.1016/j.ccl.2021.02.063](https://doi.org/10.1016/j.ccl.2021.02.063).

References

- [1] H. Oh, M. Hirscher, *Eur. J. Inorg. Chem.* (2016) 4278–4289.
- [2] S. Niimura, T. Fujimori, D. Minami, et al., *J. Am. Chem. Soc.* 134 (2012) 18483–18486.
- [3] J. Cai, Y. Xing, X. Zhao, *RSC Adv.* 2 (2012) 8579–8586.
- [4] J.Y. Kim, H. Oh, H.R. Moon, *Adv. Mater.* 31 (2019) 1805293.
- [5] R. Bhattacharyya, K. Bhanja, S. Mohan, *Int. J. Hydrog. Energy* 41 (2016) 5003–5018.
- [6] A. Lazar, S. Brad, M. Vijulie, A. Oubraham, *Fusion Eng. Des.* 146 (2019) 1998–2001.
- [7] F. Huang, *Int. J. Hydrog. Energy* 43 (2018) 1718–1724.
- [8] H.K. Rae, *Selecting Heavy Water Processes*, ACS Symposium Series, Washington D.C., 1978.
- [9] X. Deng, D. Luo, C. Qin, et al., *Int. J. Hydrog. Energy* 44 (2019) 16675–16683.
- [10] M.V. Ananyev, A.S. Farlenkov, E.K. Kurumchin, *Int. J. Hydrog. Energy* 43 (2018) 13373–13382.
- [11] J.J.M. Beenakker, V.D. Borman, S.Y. Krylov, *Chem. Phys. Lett.* 232 (1995) 379–382.
- [12] H. Tanaka, H. Kanoh, M. Yudasaka, S. Iijima, K. Kaneko, *J. Am. Chem. Soc.* 127 (2005) 7511–7516.
- [13] X.Z. Chu, Z.P. Cheng, Y.J. Zhao, et al., *Sep. Purif. Technol.* 146 (2015) 168–175.
- [14] X. Zhao, S. Villar-Rodil, A.J. Fletcher, K.M. Thomas, *J. Phys. Chem. B* 110 (2006) 9947–9955.
- [15] Y. Xing, J. Cai, L. Li, M. Yang, X. Zhao, *Phys. Chem. Chem. Phys.* 16 (2014) 15800–15805.
- [16] J. Perez-Carbajo, J.B. Parra, C.O. Ania, P.J. Merklings, S. Calero, *ACS Appl. Mater. Interfaces* 11 (2019) 18833–18840.
- [17] J.M. Salazar, S. Lectez, C. Gauvin, et al., *Int. J. Hydrog. Energy* 42 (2017) 13099–13110.
- [18] R. Xiong, R.B. Xicohtencatl, L. Zhang, et al., *Microporous Mesoporous Mater.* 264 (2018) 22–27.
- [19] J.Y. Kim, L. Zhang, R. Balderas-Xicohtencatl, et al., *J. Am. Chem. Soc.* 139 (2017) 17743–17746.
- [20] L. Zhang, S. Jee, J. Park, et al., *J. Am. Chem. Soc.* 141 (2019) 19850–19858.
- [21] J. Teufel, H. Oh, M. Hirscher, et al., *Adv. Mater.* 25 (2013) 635–639.
- [22] D. Cao, H. Huang, Y. Lan, et al., *J. Mater. Chem. A* 6 (2018) 19954–19959.
- [23] D. Cao, J. Ren, Y. Gong, et al., *J. Mater. Chem. A* 8 (2020) 6319–6327.
- [24] H. Oh, S.B. Kalidindi, Y. Um, et al., *Angew. Chem. Int. Ed.* 52 (2013) 13219–13222.
- [25] M. Liu, L. Zhang, M.A. Little, et al., *Science* 366 (2019) 613–620.
- [26] S.A. FitzGerald, C.J. Pierce, J.L.C. Rowsell, E.D. Bloch, J.A. Mason, *J. Am. Chem. Soc.* 135 (2013) 9458–9464.
- [27] Q. Li, J. Duan, W. Jin, *Chin. Chem. Lett.* 29 (2018) 854–856.
- [28] W. Fan, Y. Wang, Z. Xiao, et al., *Chin. Chem. Lett.* 29 (2018) 865–868.
- [29] Y.P. Xia, C.X. Wang, M.H. Yu, X.H. Bu, *Chin. Chem. Lett.* 32 (2021) 1153–1156.
- [30] X. Wang, Y. Wang, K. Lu, W. Jiang, F. Dai, *Chin. Chem. Lett.* 32 (2021) 1169–1172.
- [31] I. Weinrauch, I. Savchenko, D. Denysenko, et al., *Nat. Commun.* 8 (2017) 14496.
- [32] S.A. FitzGerald, D. Mukasa, K.H. Rigdon, N. Zhang, B.R. Barnett, *J. Phys. Chem. C* 123 (2019) 30427–30433.
- [33] H. Oh, I. Savchenko, A. Mavrandonakis, T. Heine, M. Hirscher, *ACS Nano* 8 (2014) 761–770.
- [34] Y. Si, X. He, J. Jiang, et al., *Nano Res.* 14 (2021) 518–525.
- [35] Y. Si, W. Wang, E.S.M. El-Sayed, D. Yuan, *Sci. China Chem.* 63 (2020) 881–889.
- [36] M.T. Kapelewski, S.J. Geier, M.R. Hudson, et al., *J. Am. Chem. Soc.* 136 (2014) 12119–12129.
- [37] H.-M. Wen, H. Wang, B. Li, et al., *Inorg. Chem.* 55 (2016) 7214–7218.
- [38] A.L. Myers, J.M. Prausnitz, *AIChE J.* 11 (1965) 121–127.
- [39] D. Noguchi, H. Tanaka, A. Kondo, et al., *J. Am. Chem. Soc.* 130 (2008) 6367–6372.